Negative Droplets from Positive Electrospray

Joshua T. Maze, Thaddeus C. Jones, and Martin F. Jarrold*

Chemistry Department, Indiana University, 800 East Kirkwood Avenue, Bloomington, Indiana 47405

Image charge detection has been used to measure the charge and velocity of individual electrosprayed water droplets. With a positive bias on the electrospray needle the majority of the droplets are, as expected, positively charged. However, a small fraction, surprisingly, carry a negative charge. Plausible explanations for the presence of the negatively charged droplets are discussed. In particular, we consider the possibility of the negatively charged droplets resulting from a bipolar fission process where the incorporation of a small negatively charged droplet between two larger positively charged progeny lowers the energy barrier for symmetric fission.

Introduction

Charged liquid droplets play an important role in many phenomena, ranging from the charging of thunderstorms[1-3] to electrospray ionization.[4-8] They become unstable when the electrostatic forces exceed the surface tension. Rayleigh investigated this instability many years ago by considering whether small distortions from spherical were stabilizing or destabilizing.[9,10] This analysis led to the now well-known Rayleigh limit for the stability of charged droplets:

$$q_R = 4\pi[(n + 2)\epsilon_0\gamma r^3]^{1/2} \qquad (1)$$

where q_R is the charge on the droplet, r is the radius, γ is the surface energy, and n indicates the number of lobes in the deformed drop. The quadrupole (prolate/oblate) distortion with $n = 2$ becomes unstable at the lowest charge. The unstable droplets may fission into two or more progeny with roughly equal size, explode into many small droplets,[11] or discharge by emitting a fine jet of charged nanodroplets.[12-16] Such jets have been imaged for levitated microdroplets.[13,16-19] While larger charged microdroplets discharge by emitting jets, smaller droplets are expected to undergo a fission process. Explosion into many small progeny appears to be a property of droplets charged substantially above the Rayleigh limit.[11,20]

Fragmentation is a ubiquitous process, and the ideas developed for the stability of liquid droplets have found applications in related problems including nuclear fission,[21,22] the stability of multiply charged metal clusters,[23-27] the gas-phase dissociation of protein complexes,[28-33] and the expansion of optical molasses.[34] In this paper we report results obtained using image charge detection[35-40] to examine the droplets generated by electrospraying pure water. Charge and velocity distributions have been recorded for electrosprayed water droplets that are transmitted through a capillary interface into vacuum. Surprisingly, we find that a small fraction of the droplets generated by positive electrospray are negatively charged. Using a simple model we explore the idea that the negatively charged droplets result from a bipolar fission process where a positively charged droplet breaks into two positively charged droplets and a small negatively charged one. The small negatively charged droplet,

* Author to whom correspondence should be addressed. E-mail: mfj@indiana.edu.
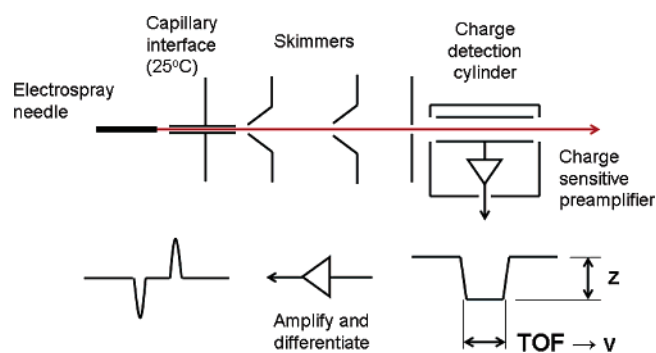
Figure 1. Schematic diagram of the experimental apparatus.

which sits between the two larger positively charged droplets, lowers the energy barrier for fission.

Experimental Methods

A schematic diagram of the experiment is shown in Figure 1. Droplets are generated by electrospray of purified (18.2 MΩ) and filtered (20 nm filter) water. The electrospray needle is a polyimide-coated fused silica capillary (Polymicro) with an inner diameter of 250 μm. Droplets enter the vacuum chamber through a 500 μm inner diameter stainless steel capillary that is embedded in a copper block. The copper block is gently heated with electrical heaters to 25−30 °C. The electrospray needle was held 2−5 mm from capillary interface, and the flow rate was ∼0.20 mL/h. The capillary interface is grounded. Droplets are produced by applying a potential of +4.5 kV to the water in the electrospray needle. The electrospray current was around 0.35 μA. The exit of the stainless steel capillary is 3 mm from the first of two conical skimmers that are separated by 28 mm. The pressure in the region behind the first skimmer (which is pumped by a mechanical booster pump) is ∼0.40 Torr. The pressure behind the second skimmer is ∼8 × 10^{-5} Torr. Both skimmers are grounded. The final stage of the instrument (2 × 10^{-6} Torr) houses the charge detection assembly which is modeled after the design of Fuerstenau and Benner.[38] The charge detection cylinder has a length of 38.1 mm and an inner diameter of 6.5 mm. When droplets enter the cylinder they impress on it an equal and opposite image charge. The cylinder is connected to a low-noise charge-sensitive preamplifier (Amptek A250 with an external 2SK152 JFET). The cylinder and preamplifier are
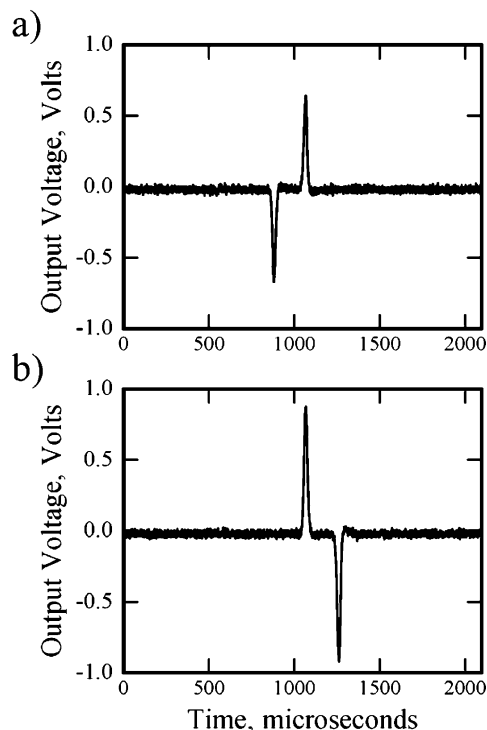
Figure 2. Examples of transients recorded for (a) a positively charged droplet and (b) a negatively charged droplet.

Figure 3. The upper plots show histograms of the charge distributions and velocity distributions of the droplets generated by positive electrospray. The results for positive droplets are shown in red. Negative droplets ($\times 100$) are shown in blue. The lower plot is a scatter plot of charge against velocity showing the correlation between these two quantities. Positively charged droplets are red, and negatively charged droplets are blue.

surrounded by a grounded case which has 5 mm diameter entrance and exit apertures which allow droplets to pass through the charge detection cylinder. The charge detection assembly is preceded by a thin plate with a 1 mm aperture which collimates the droplet beam. The signal from the preamplifier is taken out of the vacuum chamber where it is amplified and differentiated (Ortec, 571) and then presented to a transient digitizer (Alazartech, ATS460). The transient digitizer is programmed to trigger on droplet signals above a preset threshold. We typically record 10 000 transients, which are then sorted and analyzed off-line.

Experimental Results

The transient from a single positively charged droplet is shown in Figure 2a. The initial negative-going pulse results from the droplet entering the cylinder, and the subsequent positive-going one results from the droplet leaving. The time between the two pulses (along with the effective length of the cylinder[41]) gives the velocity of the droplet. The area enclosed by the pulses is proportional to the charge. The proportionality constant is determined by applying a small voltage pulse to a known capacitance at the input of the preamplifier.

In addition to traces that show a single droplet, as in Figure 2a, many traces have peaks due to two or more closely spaced droplets, which may result from the breakup of larger droplets upstream from the charge detection cylinder. This breakup could occur as the droplets travel between the electrospray needle and the capillary interface, as they travel through the capillary interface, or after the droplets enter the vacuum chamber. In a vacuum, rapid evaporative cooling will supercool the droplets, and they may subsequently freeze.[42] During evaporative cooling, the droplet diameters will shrink by about 5%,[43] which is probably enough for some droplets to exceed the Rayleigh limit. These droplets may fission or discharge before they dissociate. Once the droplets freeze, dissociation will become much more difficult since it will require the cleavage of a small ice crystal.

The vast majority of the droplets are positively charged. Positive electrospray is expected to yield positively charged droplets. The strong electric field at the end of the electrospray needle polarizes the water and leads to the formation of a Taylor cone which emits positively charged droplets.[6,8] It is difficult to imagine that a negatively charged droplet could leave the Taylor cone under these circumstances. Despite this we find that a small fraction (typically around 1% under the conditions employed here) of the droplets that pass through the detector are negatively charged. An example of the transient for a negatively charged droplet is shown in Figure 2b. It is similar to Figure 2a except that the polarities of the two peaks are reversed. We stress here that there is no voltage in the experimental apparatus beyond that applied to the electrospray needle. Everything else, including the capillary interface, is grounded. A reviewer suggested the possibility that the negatively charged droplets could arise from discharge events. To address this question we monitored the voltage on the electrospray needle with a fast transient digitizer while another transient digitizer recorded the signal from the droplets. We found that discharge events were rare and not correlated with the negative droplets.

The upper half of Figure 3 shows examples of histograms of the charge and velocity distributions obtained for isolated droplets from a typical data set. The voltage threshold for the transient digitizer was set to a value corresponding to a charge of around 5000 elementary charges (e) (8.0×10^{-16} C) for this data set. The charge distribution for the positively charged droplets (shown in red) appears to be roughly exponential. For the negatively charged droplets, where the abundances are scaled up by a factor of 100, only the low charges are observed. The velocity distribution for the positively charged droplets appears to be roughly Gaussian. The distribution is centered around 275 ms^{-1}, and extends from ~ 150 ms^{-1} to ~ 450 ms^{-1}. The velocity distribution for the negatively charged droplets is peaked at a slightly lower velocity than the positively charged ones. The lower half of Figure 3 shows a plot of charge against velocity for the positive (red) and negative (blue) droplets. There is

Negative Droplets from Positive Electrospray

J. Phys. Chem. A, Vol. 110, No. 46, 2006 **12609**

clearly some correlation between the charge and velocity. The fastest moving droplets all have relatively low charges.

Discussion

The droplets are accelerated as they travel through the capillary interface and in the expansion at the end of the capillary. The average flow velocity in the capillary is in excess of 180 ms^{-1} (based on the gas flow through the capillary). The terminal flow velocity for a perfect isentropic expansion of air at 300 K is 780 ms^{-1}. However, the expansion at the end of the capillary is relatively mild, and the terminal flow velocity will not be this high. The droplet velocities range from 150 to 450 ms^{-1}. Some of this distribution probably results from velocity slip within the expansion. Heavier molecules in a seeded supersonic expansion are often not accelerated to the full velocity of the carrier.[44] Since the droplets studied here probably have diameters that range up to several micrometers, some velocity slip is expected. The correlation between the charge on the droplets and their velocity supports this interpretation. The more highly charged droplets (which are presumably also the larger droplets) have velocities at the low end of the distribution (200−300 ms^{-1}), while those with low charge and high velocities (350−450 ms^{-1}) are probably the smaller droplets.

The most intriguing result reported here is the observation that around 1% of the droplets passing through the detector are negatively charged when the electrospray needle is at +4.5 kV. It is difficult to imagine a negatively charged droplet leaving the electrospray needle when it is biased at such a large positive voltage. Negatively charged droplets would be attracted back to the electrospray needle by the very strong electric field around the needle. Thus the negatively charged droplets must result from the positively charged droplets after they enter the capillary interface.

To a first approximation, the energy of a charged, conducting, spherical droplet can be thought of as being composed of the electrostatic energy and the surface energy:

$$E = \frac{z^2 e^2}{8\pi\epsilon_0 r} + 4\pi r^2 \gamma \tag{2}$$

where r is the radius, ze the charge, and γ the surface energy. The energies of possible fragmentation pathways can be obtained by summing the energies of the progeny, subject to the constraints of conservation of charge and volume. At low charge, the parent droplet is stable (because both symmetric and asymmetric fission increase the surface energy), but with increasing charge the parent becomes unstable toward asymmetric fission (the products of asymmetric fission become lower in energy than the parent). This occurs at around 50% of the Rayleigh limit. At around 70% of the Rayleigh limit the products of symmetric fission become lower in energy than those of asymmetric fission. With increasing charge it becomes energetically more favorable to break apart into three equal-sized progeny rather than two, and then, at the Rayleigh limit, four.[36] Ultimately, as the charge is raised further and further above the Rayleigh limit, explosion into many small progeny becomes the most energetically favored fragmentation route.[11,20]

In experimental studies, however, the droplets do not fission into a few roughly equal-sized progeny or even explode into many roughly equal-sized progeny. Instead, they discharge at close to the Rayleigh limit[45] by emitting a jet of charged nanodroplets. In this process the charge is substantially reduced (by around 10−25%) with only a small decrease in the mass
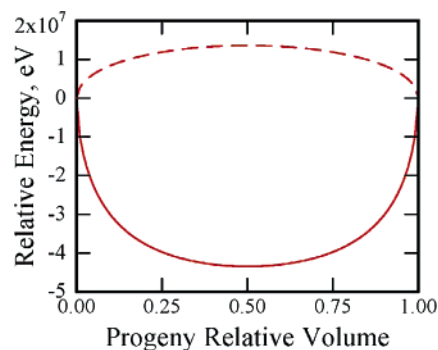
Figure 4. The solid red line shows a plot of energy difference between a parent and two progeny droplets as a function of the relative volume of the progeny. The energy difference was obtained by minimizing eq 4 in the text subject to conservation of volume and charge. The dashed line shows the result of incorporating the energy barrier according to eq 3 in the text. The results are for a parent droplet with $r_P = 4.0\ \mu$m at the Rayleigh limit ($z_P = 10^6$ e).

(negligible to 5%). This occurs because there is an energy barrier for droplet fission. If two positively charged droplets are brought together they repel each other. A rough estimate of the barrier associated with this repulsion can be obtained by considering the electrostatic energy for two spherical droplets separated by an infinitesimal distance.[22] The energy barrier is then

$$\Delta E_B = \Delta E + \frac{z_1 z_2 e^2}{4\pi\epsilon_0 (r_1 + r_2)} \tag{3}$$

where ΔE is the energy difference between the parent droplet and two progeny droplets at infinity:

$$\Delta E = \left[\frac{z_P^2 e^2}{8\pi\epsilon_0 r_P} + 4\pi r_P^2 \gamma\right] - \left[\frac{z_1^2 e^2}{8\pi\epsilon_0 r_1} + 4\pi r_1^2 \gamma\right] - \left[\frac{z_2^2 e^2}{8\pi\epsilon_0 r_2} + 4\pi r_2^2 \gamma\right] \tag{4}$$

In eq 4, the first term in square brackets is the electrostatic and surface energies of the parent droplet, while the second and third square brackets are the same for the two progeny droplets. ΔE and ΔE_B depend on the charge of the two progeny droplets (z_1 and z_2) and on their radii (r_1 and r_2). z_1 and z_2 are constrained by conservation of charge in the fragmentation process, and r_1 and r_2 are constrained by conservation of the parent droplet volume.

The result of minimizing ΔE as a function of the progeny relative volume, subject to the constraints mentioned above, is shown as the solid red line in Figure 4. The results shown in the figure are for a droplet with $r_P = 4\ \mu$m at the Rayleigh limit ($z_P = 10^6$). Symmetric fission into two equally sized progeny droplets is the lowest energy fragmentation process. The dashed line in Figure 4 shows the result of adding repulsion between the progeny droplets to give the energy barrier according to eq 3. Symmetric fission has the highest energy barrier, while the barrier vanishes in the asymmetric fission limit (i.e. fragmentation into one very large and one very small droplet). The products generated by this process are not as low in energy as in symmetric fission. However, the energy barrier is lower and sequential loss of many small droplets will discharge the parent droplet because the charge-to-volume ratio of the small droplets is much greater than for the large one. This is equivalent to the jetting process that has been observed for large microdroplets. The substantial energy barrier to
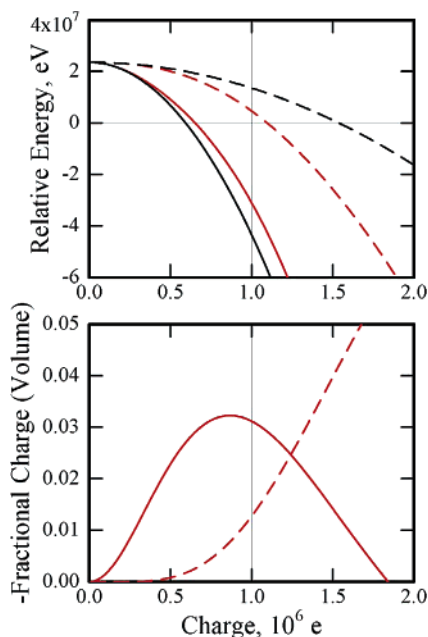
Figure 5. The upper plot shows the energies of the fission fragments from a parent droplet with $r_P = 4$ μm plotted against the total charge. The energies are relative to the energy of the parent droplet. The Rayleigh limit is at 10^6 e. The solid black line shows the energy change for symmetric fission. The dashed black line shows the energy barrier for symmetric fission obtained by incorporating the electrostatic repulsion (see text). The solid red and dashed red lines show the energy difference and energy barrier, respectively, for the optimized three droplet $+ - +$ system. The lower plot shows the charge and volume of the central droplet of the optimized three droplet system. The solid red line shows $-$fractional charge plotted against the charge on the parent droplet, and the dashed red line shows the relative volume.

symmetric fission is why fission has not been observed for microdroplets.

The energy barrier for droplet fission can be lowered by incorporating a small negatively charged droplet between the two positively charged fission fragments. If a negatively charged droplet is created, the charge on the two positively charged progeny must increase so that the overall charge is conserved. The energy of the three droplet system is given by the sum of their charging energies and surface energies, while the energy barrier now incorporates the repulsive and attractive electrostatic interactions between the three $+ - +$ droplets. For a parent droplet at the Rayleigh limit, the electrostatic interactions between the $+ - +$ progeny droplets can be made attractive rather than repulsive if a sufficiently large negative charge is placed on the central droplet. However, the large increase in the charge that is needed to make the overall electrostatic interaction attractive leads to a substantial increase in the charging energy so that dissociation along this pathway is energetically unfavorable. On the other hand, there are situations where the decrease in the unfavorable electrostatic interactions outweighs the increase in the charging energies, and the overall energy barrier is decreased compared to that for fission into two positively charged droplets. To identify the most favorable situation, we minimized the energy barrier as a function of the charge and volume of the central droplet, assuming that the charge and volume of the two larger, positively charged progeny are equal to each other. The results are plotted in Figure 5 for a parent droplet with $r_P = 4$ μm which has a Rayleigh limit of $z_P = 10^6$.

The upper half of Figure 5 shows the relative energy plotted against charge. All energies are relative to the parent droplet.

The solid black line shows the energy change for symmetric fission. The positive value at zero charge reflects the increase in the surface energy for splitting into two equally sized droplets. The relative energy decreases with increasing charge because of the decrease in the electrostatic energy of the progeny droplets relative to the parent. Fission becomes energetically favorable (relative energy becomes <0) at a charge ~60% of the Rayleigh limit (which is at 10^6 e). The black dashed line shows the energy barrier (eq 3) obtained by incorporating the electrostatic repulsion between the two spherical progeny droplets separated by an infinitesimal distance. The solid red and dashed red lines show, respectively, the energy difference for the optimized three droplet $+ - +$ system and the corresponding energy barrier. The energy barrier is significantly lowered by fission into three $+ - +$ droplets instead of two positively charged droplets. The lower half of Figure 5 shows a plot of the optimized $-$fractional charge (solid line) and fractional volume (dashed line) for the middle of the three $+ - +$ droplets. A fractional charge of -0.02 on the middle droplet indicates fractional charges of $+0.51$, -0.02, and $+0.51$ on the droplets, relative to the charge of 10^6 e on the parent droplet. Within the framework of the simple model employed here the energy barrier at the Rayleigh limit is minimized with a fractional charge of around 0.03 and a fractional volume for the middle droplet of around 0.01.

We do not pretend that this model gives an accurate quantitative description, but we believe that it captures the essential physics of the problem. It shows that the energy barrier for symmetric fission can be substantially reduced by incorporating a small negatively charged droplet between the two larger positively charged progeny. However, while this bipolar fission process lowers the activation barrier for symmetric fission, asymmetric fission still has a lower activation barrier at the Rayleigh limit. The barrier for asymmetric fission (to produce two positively charged progeny) approaches zero as the smaller droplet becomes vanishingly small. For bipolar fission the energy barrier vanishes (and becomes <0) for droplets charged to less than 10% over the Rayleigh limit, compared to more than 50% over the Rayleigh limit for symmetric fission into two positively charged droplets. So bipolar fission becomes competitive with asymmetric fission for droplets charged to less than 10% over the Rayleigh limit. The rapid evaporative cooling that occurs for droplets in a vacuum could drive some of them to more than 10% over the Rayleigh limit. So it is plausible that bipolar fission can account for the negative droplets found here. The crude model used here almost certainly overestimates the energy barriers for symmetric fission because we do not consider the polarization of the progeny droplets (where one droplet polarizes the other).

In the experiments, the negatively charged droplets have charges of around $-(2-3) \times 10^4$ e. If this corresponds to around 3% of the total charge, then the parent droplet charge must be around 10^6 e. The next obvious question is where does the negative charge arise from? The excess positive charge on the droplet is presumably due to H_3O^+. The H_3O^+ is expected to lie on the surface of the droplet, leaving the core uncharged. The water in the core of the droplet will self-ionize according to

$$H_2O_{(l)} + H_2O_{(l)} \leftrightarrow H_3O^+_{(aq)} + OH^-_{(aq)} \qquad (5)$$
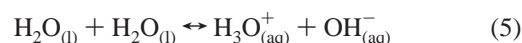
and the resulting OH^- could be the source of the negative charge. Using the ionization constant of water ($K_w = [H_3O^+_{(aq)}][OH^-_{(aq)}] = 10^{-14}$ at STP) there are expected to be around 1.6×10^4 H_3O^+/OH^- pairs in a droplet with a radius of

4 μm. Thus if there is no further ionization during the dissociation process, virtually all of the OH$^-$ generated by self-ionization must be localized in the negatively charged droplet. The driving force for this charge localization is the lowering of the energy barrier to fission.

Are there other plausible explanations for the presence of the negatively charged droplets? Neutral or lightly charged droplets can be induced to discharge when placed in a strong electric field.[46−49] The discharge process appears to involve the formation of a sharp protuberance on the droplet. For the neutral droplet, the discharge occurs at a field known as the Taylor limit:

$$E_T = \frac{c}{(8\pi)^{1/2}}\left(\frac{2\gamma}{\epsilon_0 r}\right)^{1/2} \tag{6}$$

where c is a dimensionless constant (1.625). Charged droplets discharge at a lower field. In a recent paper, Beauchamp and collaborators reported that lightly charged (3−13% of the Rayleigh limit) 225 μm methanol droplets would change polarity when exposed to a field above the Taylor limit.[50] In other words, a positively charged droplet will undergo a discharge event leaving it negatively charged. It is plausible that this could occur in the field between the electrospray needle and the capillary interface (the only place in the experiment where there is a significant electric field). However, the droplets studied here are smaller than Beauchamp's, and water has a higher surface energy than methanol, so that the field required to induce a similar polarity change in the droplets studied here is substantially larger, and in fact several times the breakdown voltage of air. Even if this process did occur, the resulting negatively charged droplet would be attracted back to the electrospray needle. Thus field induced polarity changes can be ruled out as the origin of the negative droplets.

Another process that we should consider as a potential source of negatively charged droplets is collision with metal surfaces. For example, charged droplets could collide with the walls of the capillary interface, with the skimmers, or with the collimating plate placed before the image charge detector. The collisions that occur with the skimmers and the collimating plate will be quite energetic because the droplets are traveling at several hundreds of meters per second. These collisions may directly fragment the droplets or cause substantial heating, which will lead to further evaporative cooling and dissociation, if the droplets exceed the Rayleigh limit. It is also possible that collisions with the metal surface will partially discharge the droplets. It is not clear how these collisions could directly lead to the formation of negatively charged droplets; however, we cannot completely rule out this possibility.

Finally, another possible source of the negatively charged droplets, that should be mentioned, is turbulence within the capillary interface. Turbulence will presumably help the droplets to break apart at a charge lower than the Rayleigh limit. It is not clear how turbulence could lead to negative droplet formation, but again we cannot completely rule out this possibility.

Summary and Conclusions

We have used image charge detection to investigate the charge and velocity of electrosprayed water droplets transmitted through a capillary interface. Surprisingly, we find that a small fraction ($\sim$1%) of the droplets that reach the detector are negatively charged. Using a crude model we have explored the possibility that the negatively charged droplets result from a bipolar fission process where the incorporation of a small negatively charged droplet between two larger positively charged fission fragments lowers the energy barrier to fission. According to the model, bipolar fission becomes competitive with asymmetric fission for droplets charged to less than 10% over the Rayleigh limit. More sophisticated simulations, that include polarization, are required to fully evaluate the feasibility of this process. We also consider the possibility of the negatively charged droplets resulting from field induced polarity changes, from high energy collisions of the droplets with metal surfaces, and from turbulence within the capillary interface.

References and Notes

(1) Reynolds, S. E.; Brooks, M.; Foulks Gourley, M. Thunderstorm Charge Separation. *J. Meteorol.* **1957**, *14*, 426−436.

(2) Bürgesser, R. E.; Pereyra, R. G.; Avila, E. E. Charge Separation in Updraft of Convective Regions of Thunderstorms. *Geophys. Res. Lett.* **2006**, *33*, L03808.

(3) Sherwood, S. C.; Phillips, V. T. J.; Wettlaufer, J. S. Small Ice Crystals and the Climatology of Lightning. *Geophys. Res. Lett.* **2006**, *33*, L05804.

(4) Fenn, J. B.; Mann, M.; Meng, C. K.; Wong, S. F.; Whitehouse, C. M. Electrospray Ionization for Mass Spectrometry of Large Biomolecules. *Science*, **1989**, *246*, 64−71.

(5) Fenn, J. B.; Mann, M.; Meng, C. K.; Wong, S. F.; Whitehouse, C. M. Electrospray Ionization—Principles and Practice. *Mass Spectrom. Rev.* **1990**, *9*, 37−70.

(6) Cole, R. B. Some Tenets Pertaining to Electrospray Ionization Mass Spectrometry. *J. Mass Spectrom.* **2000**, *35*, 763−772.

(7) Gamero-Castaño, M.; Fernandez de la Mora, J. Kinetics of Small Ion Evaporation and Mass Distribution of Multiply Charged Clusters in Electrosprays. *J. Mass Spectrom.* **2000**, *35*, 790−803.

(8) Kebarle, P. A Brief Overview of the Present Status of the Mechanisms Involved in Electrospray Mass Spectrometry. *J. Mass Spectrom.* **2000**, *35*, 804−817.

(9) Lord Rayleigh, On the Equilibrium of Liquid Conducting Masses Charged with Electricity. *Philos. Mag.* **1882**, *14*, 184−186.

(10) Hendricks, C. D.; Schneider, J. M. Stability of a Conducting Droplet under the Influence of Surface Tension and Electrostatic Forces. *Am. J. Phys.* **1963**, *31*, 450−453.

(11) Last, I.; Levy, Y.; Jortner, J. Beyond the Rayleigh Instability Limit for Multicharged Finite Systems: From Fission to Coulomb Explosion. *Proc. Natl. Acad. Sci. U.S.A.* **2002**, *99*, 9107−9112.

(12) Taflin, D. C.; Ward, T. L.; Davis, E. J. Electrified Droplet Fission and the Rayleigh Limit. *Langmuir* **1989**, *5*, 376−384.

(13) Gomez, A.; Tang, K. Charge and Fission of Droplets in Electrostatic Sprays. *Phys. Fluids* **1994**, *6*, 404−414.

(14) Feng, X.; Bogan, M. J.; Agnes, G. R. Coulomb Fission Event Resolved Progeny Droplet Production from Isolated Evaporating Methanol Droplets. *Anal. Chem.* **2001**, *73*, 4499−4507.

(15) Smith, J. N.; Flagan, R. C.; Beauchamp, J. L. Droplet Evaporation and Discharge Dynamics in Electrospray Ionization. *J. Phys. Chem. A* **2002**, *106*, 9957−9967.

(16) Duft, D.; Achtzehn, T.; Muller, R.; Huber, B. A.; Leisner, T. Coulomb Fission − Rayleigh Jets from Levitated Microdroplets. *Nature* **2003**, *421*, 128−128.

(17) Hager, D. B.; Dovichi, N. J. Behavior of Microscopic Liquid Droplets Near a Strong Electrostatic Field, Droplet Electrospray. *Anal. Chem.* **1994**, *66*, 1593−1594.

(18) Hager, D. B.; Dovichi, N. J.; Klassen, J. S.; Kebarle, P. Droplet Electrospray Mass Spectrometry. *Anal. Chem.* **1994**, *66*, 3944−3949.

(19) Grimm, R. L.; Beauchamp, J. L. Dynamics of Field-Induced Droplet Ionization: Time-Resolved Studies of Distortion, Jetting, and Progeny Formation from Charged and Neutral Methanol Droplets Exposed to Strong Electric Fields. *J. Phys. Chem. B* **2005**, *109*, 8244−8250.

(20) Cahn, J. W. Stability of Electrically Charged Conducting Droplets, *Phys. Fluids* **1962**, *5*, 1662−1663.

(21) Meitner, L.; Frisch, O. R. Disintegration of Uranium by Neutrons: a New Type of Nuclear Reaction. *Nature (London)* **1939**, *143*, 239−240.

(22) Bohr, N.; Wheeler, J. A. The Mechanism of Nuclear Fission. *Phys. Rev.* **1939**, *56*, 426−450.

(23) Sattler, K.; Mühlbach, J.; Echt, O.; Pfau, P.; Recknagel E. Evidence for Coulomb Explosion of Doubly Charged Microclusters. *Phys. Rev. Lett.* **1981**, *47*, 160−163.

(24) Bréchignac, C.; Cahuzac, Ph.; de Frutos, M.; Kebaïli, N.; Sarfati, A.; Akulin, V. Experimental Evidence for the Entropy Effect in Coulombic Cluster Fission. *Phys. Rev. Lett.* **1996**, *77*, 251−254.

(25) Echt, O.; Märk, T. D. In *Clusters of Atoms and Molecules II*, Haberland, H., Ed.; Springer: New York, 1994.

(26) Näher, U.; Bjørnholm, S.; Frauendorf, S.; Garcias, F.; Guet, C. Fission of Metal Clusters. *Phys. Rep.* **1997**, *285*, 245−320.

(27) Chandezon, F.; Tomita, S.; Cormier, D.; Grübling, P.; Guet, C.; Lebius, H.; Pesnelle, A.; Huber, B. A. Rayleigh Instabilities in Multiply Charged Sodium Clusters. *Phys. Rev. Lett.* **2001**, *87*, 153402.

(28) Light-Wahl, K. J.; Schwartz, B. L.; Smith, R. D. Observation of the Non-Covalent Quaternary Associations of Proteins by Electrospray Ionization. *J. Am. Chem. Soc.* **1994**, *116*, 5271.

(29) Versluis, C.; Heck, A. J. R. Gas-Phase Dissociation of Hemoglobin. *Int. J. Mass Spectrom.* **2001**, *210/211*, 637−649.

(30) Mauk, M. R.; Mauk, A. G.; Chen, Y.-L.; Douglas, D. J. Tandem Mass Spectrometry of Protein-Protein Complexes: Cytochrome c - Cytochrome b₅. *J. Am. Soc. Mass Spectrom.* **2002**, *13*, 59−71.

(31) Benesch, J. L. P.; Sobott, F.; Robinson, C. V. Thermal Dissociation of Multimeric Protein Complexes by Using Nanoelectrospray Mass Spectrometry. *Anal. Chem.* **2003**, *75*, 2208−2214.

(32) Jurchen, J. C.; Williams, E. R. Origin of Asymmetric Charge Partitioning in the Dissociation of Gas-Phase Protein Homodimers. *J. Am. Chem. Soc.* **2003**, *125*, 2817−2826.

(33) Sobott, F.; Robinson, C. V. Characterising electrosprayed Biomolecules Using Tandem MS−The Noncovalent GroEL Chaperonin Assembly. *Int. J. Mass Spectrom.* **2004**, *236*, 25−32.

(34) Pruvost, L.; Serre, I.; Duong, H. T.; Jortner, J. Expansion and Cooling of a Bright Rubidium Three-Dimensional Optical Molasses, *Phys. Rev. A* **2000**, *61*, 053408.

(35) Hendricks, C. D. Charged Droplet Experiments, *J. Colloid Sci.* **1962**, *17*, 249−259.

(36) Pfeifer, R. J.; Hendricks, C. D. Charge to Mass Relationships for Electrohydrodynamically Sprayed Liquid Droplets. *Phys. Fluids* **1967**, *10*, 2149−2154.

(37) Stradling, G. L.; Idzorek, G. C.; Shafer, B. P.; Curling, H. L.; Collopy, M. T.; Hopkins Blossom, A. A.; Fuerstenau, S. Ultra High Velocity Impacts: Cratering Studies of Microscopic Impactes from 3 km/s to 30 km/s. *Int. J. Impact Eng.* **1993**, *14*, 719−727.

(38) Fuerstenau, S. D.; Benner, W. H. Molecular Weight Determination of Megadalton DNA Electrospray Ions Using Charge Detection Time-of-Flight Mass Spectrometry. *Rapid Commun. Mass Spectrom.* **1995**, *9*, 1528−1538.

(39) Benner, W. H. A Gated Electrostatic Ion Trap to Repetitiously Measure the Charge and m/z of Large Electrospray Ions. *Anal. Chem.* **1997**, *69*, 4162−4168.

(40) Fuerstenau, S. D.; Benner, W. H.; Thomas, J. J.; Brugidou, C.; Bothner, B.; Siuzdak, G. Mass Spectrometry of an Intact Virus. *Angew. Chem., Int. Ed.* **2001**, *40*, 542−544.

(41) The effective length of the charge detection cylinder was determined using two identical detectors separated by 11.1 cm. For individual droplets that passed through both detectors we determined the times spent in both detectors (i.e. the times between the centers of the entrance and exit pulses) along with the time spent traveling between the detectors (i.e. the time between the centers of the entrance pulses for both detectors). With this information, and knowledge of the geometry, the effective length can be determined.

(42) Huang, J.; Bartell, L. S. Kinetics of Homogeneous Nucleation in the Freezing of Large Water Clusters. *J. Phys. Chem.* **1995**, *99*, 3924−3931.

(43) Based on a rough estimate using the bulk heat capacity of water, the latent heat of evaporation, and a freezing temperature of 200 K (from ref 40).

(44) De Paul, S.; Pullman, D.; Friedrich, B. A Pocket Model of a Seeded Supersonic Expansion. *J. Phys. Chem.* **1993**, *97*, 2167−2171.

(45) Duft, D.; Lebius, H.; Huber, B. A.; Guet, C.; Leisner, T. Shape Oscillations and Stability of Charged Microdroplets. *Phys. Rev. Lett.* **2002**, *89*, 084503.

(46) Zeleny, J. Instability of Electrified Liquid Surfaces. *Phys. Rev.* **1917**, *10*, 1−6.

(47) Macky, W. A. Some Investigations on the Deformation and Breaking of Water Drops in Strong Electric Fields. *Proc. R. Soc. London, Ser. A* **1931**, *133*, 565−587.

(48) O'Konski, C. T.; Thatcher, H. C. The Distortion of Aerosol Droplets by an Electric Field. *J. Phys. Chem.* **1953**, *57*, 955−958.

(49) Taylor, G. Disintegration of Water Drops in an Electric Field. *Proc. R. Soc. London, Ser. A* **1964**, *280*, 383−397.

(50) Grimm, R. L.; Beauchamp, J. L. Dynamics of Field-Induced Droplet Ionization: Time-Resolved Studies of Distortion, Jetting, and Progeny Formation from Charged and Neutral Methanol Droplets Exposed to Strong Electric Fields. *J. Phys. Chem. B* **2005**, *109*, 8244−8250.